

# MEASUREMENT OF BEAM LOSSES AT THE AUSTRALIAN SYNCHROTRON

E. Nebot del Busto, M. Kastriotou, CERN, Geneva, Switzerland; University of Liverpool, Liverpool, UK,  
 M. J. Boland, ASCo, Clayton; The University of Melbourne,  
 P. D. Jackson, University of Adelaide, Adelaide,  
 R. P. Rasool, The University of Melbourne, Australia  
 E. B. Holzer, CERN, Geneva, Switzerland,  
 J. Schmidt, Albert-Ludwig Universitaet Freiburg, Freiburg, Germany  
 C. P. Welsch Cockcroft Institute, Warrington, Cheshire; University of Liverpool, Liverpool, UK

## Abstract

The unprecedented requirements that new machines are setting on their diagnostic systems is leading to the development of new generation of devices with large dynamic range, sensitivity and time resolution. Beam loss detection is particularly challenging due to the large extension of new facilities that need to be covered with localized detector. Candidates to mitigate this problem consist of systems in which the sensitive part of the radiation detectors can be extended over long distance of beam lines. In this document we study the feasibility of a BLM system based on optical fiber as an active detector for an electron storage ring. The Australian Synchrotron (AS) comprises a 216 m ring that stores electrons up to 3 GeV. The Accelerator has recently claimed the world record ultra low transverse emittance (below pm rad) and its surroundings are rich in synchrotron radiation. Therefore, the AS provides beam conditions very similar to those expected in the CLIC/ILC damping rings. A qualitative benchmark of beam losses in a damping ring-like environment is presented here. A wide range of beam loss rates can be achieved by modifying three beam parameters strongly correlated to the beam lifetime: bunch charge (with a variation range between 1 nA and 10 nA), horizontal/vertical coupling and of dynamic aperture. The controlled beam losses are observed by means of the Cherenkov light produced in a 365  $\mu$ m core Silica fiber. The output light is coupled to different type of photo sensors namely: Metal Semiconductor Metal (MSM), Multi Pixel Photon Counters (MPPCs), standard PhotoMultiplier (PMT) tubes, Avalanche PhotoDiodes (APD) and PIN diodes. A detailed comparison of the sensitivities and time resolution obtained with the different read-outs are discussed in this contribution.

## THE AUSTRALIAN SYNCHROTRON AS A DAMPING RING TEST FACILITY

The compact linear collider CLIC [1] foresees two 20 km main linacs accelerating electrons and positrons up to 3 TeV. In order to provide an instantaneous luminosity on the order of  $5 \cdot 10^{34} \text{ cm}^{-2} \text{ s}^{-1}$ , the beam spot at the interaction point shall reach unprecedentedly low nanometer sizes. This is only achievable with ultra low emittance beams at the entrance of the linac that account for the large

contribution coming from the particle sources, particularly the positron source, and the emittance growth budget up to the interaction point. The Damping Rings (DR) designed to cool down the CLIC beams [2] comprise a 412 m ring built of FODO cells in the long straight section and Theoretical Minimum Emittance (TME) in the arcs with the use of two half cells for dispersion suppression. Superconducting wigglers aim to decrease the damping times to the 2 ms level, values well below the 20 ms imposed by the 50 Hz CLIC repetition rate. This constrains the requirements on time response of beam instrumentation. Moreover, the low foreseen longitudinal emittances triggers a set of single bunch collective effects typically not observable in electron machines. Hence, the measurement of beam parameters on a bunch by bunch basis imposes a tighter requirement on the time resolution of the instrumentation systems.

The Australian Synchrotron (AS) [3] is a third generation light source consisting of a 100 MeV linac, a 100 MeV to 3 GeV Booster and a 3 GeV Storage Ring (SR). The SR comprises 14 Double Bend Achromat (DBA) cells where a 200 mA beam is circulated in pulses of approximately 600 ns when filling 300 out of the 360 buckets. As it is shown in table 1, there are many similarities between the parameters of the AS and the CLIC damping rings. In particular, the AS has recently measured vertical normalized emittances comparable to those expected in CLIC. Moreover, the synchrotron provides good flexibility to modify some of its nominal parameters to approach those of the DR. For instance it is feasible to reduce the pulse length to CLIC like values by keeping nominal beam charge. Hence, this facility provides a great opportunity to test and develop instrumentation targeting requirements for the DR of the future collider.

## OPTICAL FIBER BEAM LOSS MONITORS: THE EXPERIMENTAL SETUP

The use of optical fibers, once restricted to waveguides for the transport of information, is increasingly being adopted in the beam instrumentation field. The light generated inside an optical fiber due to the crossing of ionizing radiation may be used as a tool for Beam Loss Monitoring



(a) Storage Ring scrapers (far left), Beam Loss Monitors behind dipole (far right). (b) Optical fiber installed in the outer side of the bending magnet, beam from left to right (top view).

Figure 1: Beam loss monitor set-up in the AS.

Table 1: Comparison Between Some of the Parameters of the AS and CLIC DR.

Parameter	AS	CLIC DR
Energy (GeV)	3.0	2.86
Intensity (elec)	$9.0 \cdot 10^{+11}$	$1.28 \cdot 10^{+12}$
Number of bunches	300	312
Pulse length (ns)	600	156
Circ. length (m)	216	427.5
$f_{rev}$ (MHz)	1.38	0.73
Bunch spacing (ns)	2	0.5
$\gamma\epsilon_x$ (nm rad)	58708	472
$\gamma\epsilon_y$ (nm rad)	< 5	4.8

(BLM) [4, 5]. Two main advantages arise from the use of Optical fiber based BLM (OBLM) systems:

- The active ionizing radiation detector can be distributed over large sections of beam lines. This prevents missing the observation of beam losses at otherwise uncovered locations and it minimizes the number of required sensors (and hence acquisition systems) and therefore the cost of the system.
- OBLM systems can provide position reconstruction of the original location of the beam loss with resolutions down to a few tens of centimeters [6].

The light generation mechanism inside the optical fiber can be of various origins, namely: scintillation, fluorescence, thermoluminescence, radioluminescence, etc. In this contribution, we concentrate on Cherenkov light generated when charged particles cross the fiber with speed higher than the phase velocity of light in the core medium. As a reference number, the Cherenkov light generating energy thresholds for electrons and positrons (which account for the largest fraction of the charge component of the showers) crossing a quartz fiber is 186 keV [7].

Two 7 m long optical fibers with  $365 \mu\text{m}$  diameter  $\text{SiO}_2$  core were located on the horizontal plane of the outer side of the beam. A third fiber with reduced diameter core ( $200 \mu\text{m}$ ) was also available and provided the possibility to test three photo sensor within the same experiment. All three fibers were enclosed into a tube to shield from ambient light and were situated near the first bending magnet in sector 11. This location was selected as the easiest position to produce controlled beam losses since the beam scrapers are situated approximately 1.5 m upstream of the front face of this bending magnet, as shown in figure 1(a). The fiber enclosing plastic tube run parallel for the length of the magnet, as seen in Figure 1(b) and it immediately deviated upwards from the horizontal plane toward the roof of the accelerator tunnel where it was extracted to the upper level. A 14400 pixels  $3 \times 3 \text{ mm}^2$  active area Multi Pixel Photon Counter (MPPC) and a Photo Multiplier Tube (PMT) were coupled to the end of the two  $365 \mu\text{m}$  fibers. The light output of the third  $200 \mu\text{m}$  fiber was directed via focusing lens to the  $25 \mu\text{m}$  active area of an Avalanche Photo Diode (APD). The readout signals were observed via a 10 bit Analog to Digital Converter (ADC) or via fan in/fan out pulse discriminator and scaler as pulse counting mode electronics.

## SINGLE SHOT BLM CALIBRATION

The prototype OBLM system was calibrated by directing a single bunch beam onto a fully closed scraper in the SR. The first challenge to overcome was the determination of the number of charges hitting the intercepting device. The measurements of the DC current transformer were not available as the beam did not even complete a single turn from the injection point. Intensity measurements from the Booster ring and transfer lines did not provide enough accuracy due to the difficulty of a precise determination of the injection efficiencies. Moreover, the lower current beams injected into the machine reached values either near or significantly below the noise level of the current measuring in-

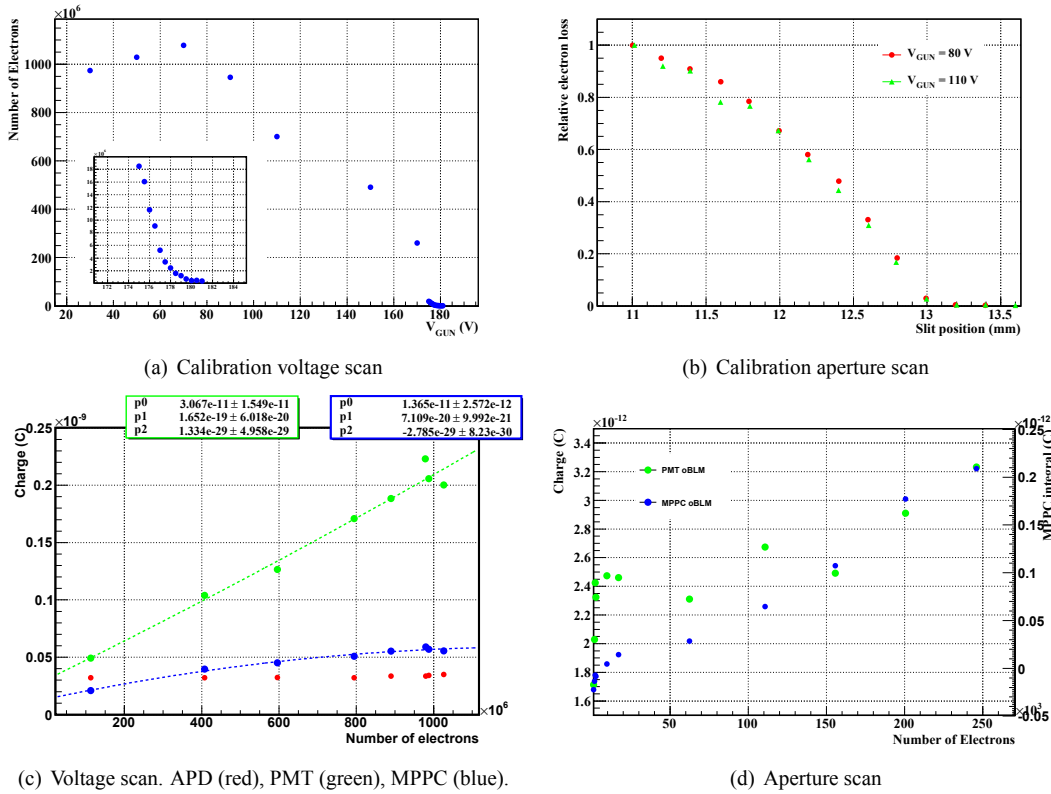


Figure 2: Beam intensity and integrated signals observed during voltage and aperture scans.

struments. Therefore, a calibration exercise was performed to determine the number of particles that could be injected in the SR in a single shot. Two parameters were modified to achieve the largest possible range, namely: the voltage of the grid in the electron gun and the position of the energy selection slits in the Booster To SR (BTS) transfer lines. For a given set of parameters, a certain number of single injections were accumulated in the SR where the intensity was measured with the DC current transformer. Thereafter, the beam was scraped out of the ring and the measurement for the subsequent set of parameters was conducted.

Figure 2(a) summarizes the results achieved during the voltage gun calibration. Note that the number of accumulated shots needed to be increased from 10 to 40 when the gun voltage was above 170 V and up to 100 above 175 V due to the non linear relation between the voltage and the number of charges. The larger number of charges corresponds to the low voltage range with a maximum at 80 V of  $1.1 \cdot 10^{+9}$  electrons. From this point the tendency is an approximately linear decrease up to voltages of 170 V. After this value a somewhat exponential decrease is observed and a minimum of  $6 \cdot 10^{+5}$  electrons is measured for  $V_{gun} = 182V$ . Similarly, Figure 2(b) presents the results of the slit grid scan. In this case the measurement was conducted for two independent gun voltages, 80 V and 110 V, to verify the reproducibility of the result. The graphic shows the charge loss relative to the upper and lower BTS slits in their nominal position, i.e. 11.0 mm.

Subsequently, a similar scan was executed with both the horizontal and vertical scrapers in the SR fully closed. Figure 3 shows the evolution of the signals over time for the three OBLMs for a gun voltage of 150 V. A single peak appears in all cases, which indicates that the position of the scrapers ensured that all the charges were fully stopped within the first turn. A clear distortion is observed on the APD signal, which was expected to provide a TTL output. This is attributed to the frequency cutoff introduced by the nearly 90 m of coaxial cables bringing the signals from the photo sensors to the ADC. The effect is also observable on the tail end of the MPPC and PMT signals, as they extend over several hundreds of nanoseconds. The performance in terms of time response of the MPPC and PMT detectors with respect to each other is inferred from the raise time of the pulse, which stands at 10 and 15 nanoseconds respectively.

In order to compare the sensitivity of the three detectors, a numerical integration of the signals acquired with the ADC was computed. Figure 2(c) presents the results obtained during the voltage scan, i.e. for injected charges ranging from 100 million to 1 billion electrons. The APD shows a flat response with beam charge. This is expected since the output of the system is a (binary) TTL signal. The tendencies of the PMT and MPPC integrals are slightly different. Even though in both cases there is an increasing behaviour, the PMT shows a more linear evolution. In both cases, a second degree polynomial was fit to the data.

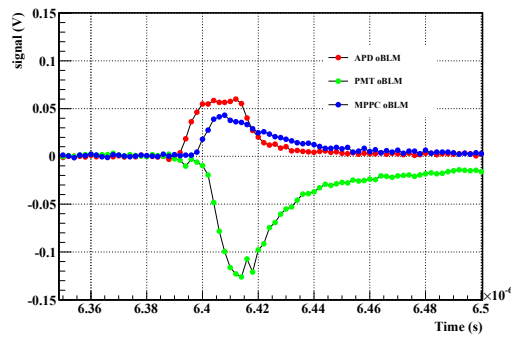


Figure 3: Signals observed in the three OBLMs during an injection of 500k electrons

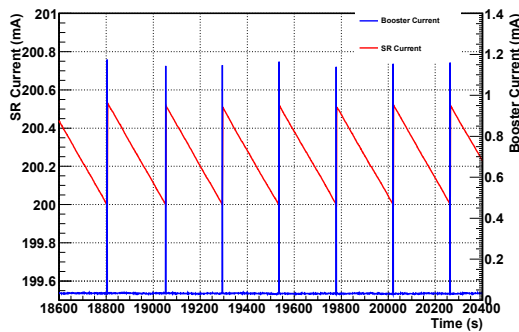


Figure 4: Booster and SR current measurement during topup injections

While the second order coefficient for the PMT is compatible with zero, the MPPC gets a clearly negative value. This is compatible with expected saturation effects when the number of incident photons exceeds the number of available pixels within the illuminated area. The summary of the results obtained for the low charge range are shown in Figure 2(d). Only the MPPC and PMT signals are shown as the APD OBLM did not observe any pulses during irradiation. This is attributed to the lower diameter core of the optical fiber for this particular OBLM<sup>1</sup> as well as to potential inefficiencies on the light coupling from the fiber to the small active area of the APD. The PMT OBLM seem to show a good linearity down to 150k electrons. This is established as the sensitivity limit with the rest of the values attributed to the dark count of the system. The MPPC signals seem to be sensitive to much lower beam charges, down to 10k electrons, despite similar expected gain. This is understood as the MPPC readout was equipped with a 30 dB amplifier in the low charge BTS scan. Moreover, this is in agreement with the more suited single photon counting capabilities of the MPPC.

ISBN 978-3-95450-141-0

## TOPUP INJECTION LOSSES

The AS works on topup mode to keep a constant nominal current of 200 mA circulating in the SR ring and continuously provide synchrotron light to the different beam lines. Figure 4 compares the intensity measurement in the SR with the fast intensity measurement performed in the Booster for 7 consecutive injections. While the SR intensities indicate an increase of 0.5 mA immediately after injection, the booster measurement provides 1.1 mA, which accounting for the Booster (SR) 216 (360) harmonic number it should provide 0.66 mA in the SR. This indicates, assuming typical injection efficiencies of 80 %, that around 0.028 mA ( $1.25 \cdot 10^{+9}$  electrons) are lost around the ring within the first several turns. The sensitivity of the OBLM system to injection losses was tested during operation of the facility by triggering on the electron gun. For this measurement, the 365  $\mu\text{m}$  fiber coupled to the PMT and MPPC detectors were compared to the signals observed by a slow *NaI* scintillator and a *NE102* plastic scintillators both coupled to PMTs and located 2 m downstream of the optical fiber.

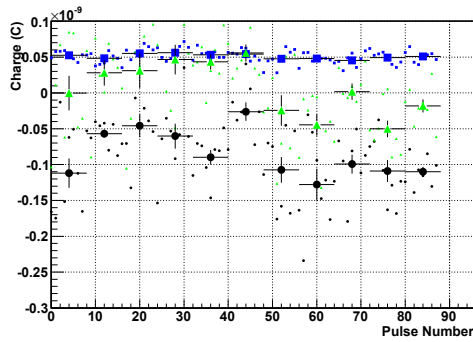
A very good shot to shot reproducibility of the signals was observed. As an example, one of the triggers is presented in Figure 5(a), where the full time range of 2 ms corresponds to 2777 turns. In all four detectors there is a clear modulation effect where the maximum of the signals peaked around every 100  $\mu\text{s}$ . This becomes more evident when performing a frequency analysis. In the power spectrum the modulation effect is clear with a 11 kHz frequency line followed by the higher order harmonics as shown in Figure 5(b). This was attributed to the synchrotron tune of the machine. Figure 5(c) presents the power spectrum in a wider range (up to 2 MHz) where some other substructure can be observed. The second most clear line that appears corresponds to 1.388 MHz which is the revolution frequency of the SR. The two side bands around  $f_{rev}$  are located at a  $\Delta f = 400$  kHz. This can be attributed to the horizontal tune of the machine. The two peaks observed around 200 kHz and 400 kHz may be also related to the horizontal and vertical tune.

## DYNAMIC APERTURE AND BETATRON COUPLING INDUCED LOSSES

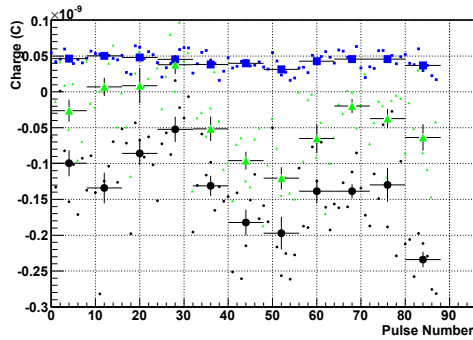
Two types of controlled losses were generated over a user-like fill, i.e. 200 mA filled within 300 RF buckets. The dynamic aperture was squeezed by changing the sextupole currents. The lifetime variation changed from 1 hour to over sixty. Despite the observation of some activity in the BLMs, no conclusion could be drawn due to the fact that the collected signals were dominated by high frequency noise picked up in the coaxial cables going from the detectors to the ADC. The skew quadrupoles settings were also modified to increase the vertical emittance from 1 pm

<sup>1</sup>In [7] it is demonstrated that the Cherenkov photon yield produced in an optical fiber is proportional to the square of the core diameter

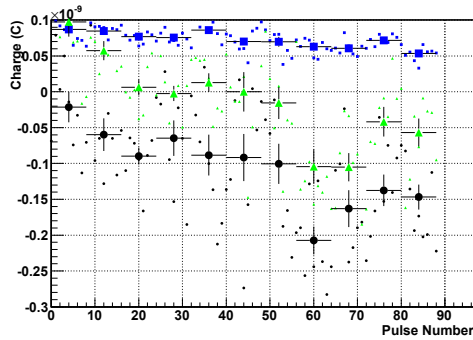




(a) Scrapper at 13mm



(b) Scrapper at 14mm



(c) Scrapper at 15mm

## REFERENCES

- [1] CLIC Collaboration, "A multi-TeV linear collider based on CLIC technology", CLIC Conceptual Design Report. Volume 1 Technical Report. CERN, Geneva 2012.
- [2] "Conceptual design of the CLIC damping Rings", Y. Papa-philippou et. al. New Orleans 2012. IPAC12.
- [3] J. Boldeman, D. Einfeld, Nucl. Instr. and Meth., A 521, 2004, p. 306-317.
- [4] "Optical Fiber Based Beam Loss Monitor for Electron Storage Rings", T. Obina. September 2013, Oxford, IBIC13.
- [5] "Fiber Optic sensors at accelerators: Considerations and Pit-falls", J. Kuhnenn, May 2013. Vienna. 3rd OPAC topical Workshop on Beam Diagnostics.
- [6] "Instrumentation for machine protection at femi@elettra", L. Froehlich et. al. Hamburg. DIPAC11.
- [7] "Cherenkov Fibers for Beam Loss Monitoring at the CLIC Two Beam Module", J. Van Hoorne, June 2012. CERN-THESIS-2012-112.

Figure 7: NaI (black), PMT-OBLM (green) and MPPC- OBLM (blue) BLM signals observed during the coupling scan. The solid points represent an average over all mea- surements for a given coupling. The small dotsshowindi- vidualmeasurements.